PCCP

Accepted Manuscript

This is an *Accepted Manuscript*, which has been through the Royal Society of Chemistry peer review process and has been accepted for publication.

Accepted Manuscripts are published online shortly after acceptance, before technical editing, formatting and proof reading. Using this free service, authors can make their results available to the community, in citable form, before we publish the edited article. We will replace this *Accepted Manuscript* with the edited and formatted *Advance Article* as soon as it is available.

You can find more information about *Accepted Manuscripts* in the Information for Authors.

Please note that technical editing may introduce minor changes to the text and/or graphics, which may alter content. The journal's standard Terms & Conditions and the Ethical guidelines still apply. In no event shall the Royal Society of Chemistry be held responsible for any errors or omissions in this *Accepted Manuscript* or any consequences arising from the use of any information it contains.

ROYAL SOCIETY OF CHEMISTRY

www.rsc.org/pccp

Novel High-Efficiency Crystalline-Silicon-Based Compound Heterojunction Solar Cells: HCT (Heterojunction with Compound Thin-layer)

Yiming Liu[1,2], Yun Sun[1]*, Wei Liu[1], Jianghong Yao[2]

[1] *Institute of Photo-electronic Thin Film Devices and Technology, Nankai University, Tianjin 300071, China*

[2] *Department of Physics, Nankai University, Tianjin 300071, China*

Abstract - With the amorphous silicon (a-Si:H)/crystalline silicon (c-Si) heterojunction structure, the Heterojunction with Intrinsic Thin-layer (HIT) solar cell has become one of the most promising technologies for c-Si based solar cells. By replacing a-Si:H thin films with appropriate compound semiconductors, we propose novel heterojunction structures which allows c-Si heterojunction solar cells to possess higher power conversion efficiencies than HIT solar cells. Several promising heterojunction candidates and hetero-structures have been proposed in this work, and this kind of novel c-Si compound heterojunction solar cell is denominated HCT (Heterojunction with Compound Thin-layer). The feasibilities of these novel HCT structures are further investigated by theoretical approaches, and the modeling results demonstrate the device performance improvements. Finally, this paper proclaims the compound selection standards and essentials of achieving high-efficiency HCT solar cells, which are guidelines for the real device implementation.

1. Introduction

The HIT solar cell has achieved an excellent power conversion efficiency of up to 24.7% on a large area of 101.8 cm^2, which demonstrates the great promise of using heterojunction techniques to achieve high efficiency c-Si based solar cells[1]. The basic structure of HIT solar cells is shown in **Fig. 1a.** So far, there have been lots of optimization efforts on improving the qualities of a-Si:H films, TCO layers and grids to pursue higher efficiency, and it turns more and more difficult to raise the efficiency through refining traditional HIT fabrication processes. To further develop the device, here arise some fundamental questions: is the a:Si:H thin film the best heterojunction partner for c-Si? Is it possible to upgrade HIT solar cells with a new heterojunction structure (as shown in **Fig. 1b**)? Prior to answer these questions, we first briefly review the role of a-Si:H played in HIT solar cells.

Different from the structure of Si homojunction solar cells[2], the c-Si wafer in HIT structure is sandwiched between nanometer-thick doped a-Si:H films with wider band gap. This heterojunction design brings about several benefits. First, it avoids the detrimental effects of band-gap narrowing and dopant-dependent mobility degradation in a highly doped homojunction

Physical Chemistry Chemical Physics Accepted Manuscript

Physical Chemistry Chemical Physics Accepted Manuscript

emitter[3]. Second, a-Si:H films not only saturate dangling bonds at the c-Si surface, but also establish reflection barriers for minority carriers at both hetero-interfaces[4] (seen in **Fig. 2a**). These barriers effectively passivate the c-Si surface recombination and also shield the recombination at the emitter contact. And third, the wider band gap of a-Si:H enlarges the quasi-Fermi level separation at heterojunction, and supports the V_{oc} enhancement[4,5]. Moreover, all the processing temperatures of HIT cells are lower than 200 °C, and the low-temperature process reduces thermal damages and device degradation[6]. However, along with the favorable effects brought by a-Si:H, it also causes blocking barriers for majority carriers at hetero-interfaces. The blocking barriers hinder the majority carrier flow through interfaces, and are not beneficial to the device performance[4]. The tunneling of majority carriers compensates for the negative effects of blocking barriers to some extent, and it is one of the reasons why a-Si:H layers need to be thin and a-Si:H of *p*-type and *n*-type are heavily doped[7–9].

Concerning the advantages and disadvantages in the energy band of HIT cells, it indicates that if replacing a-Si:H with new heterojunction materials that satisfy following criteria:

- possess even wider band gap so as to reduce parasitic light absorption[10] and assist the increment of V_{oc}[5],
- are capable of improving the interface carrier transport by increasing reflection barriers of interface minority carriers and decreasing blocking barriers of interface majority carriers (shown as **Fig. 2b**),
- still guarantee good c-Si surface passivation,

the cells with novel heterojunction partners will be allowed to obtain higher efficiency, and also inherit the advantages of using hetero-structure, such as avoiding band-gap narrowing in the homojunction emitter. Following this concept, this work attempts to explore the possibility of novel heterojunction structures described above.

2. Material Selection

As it is high-cost and not practical to test every material experimentally, reasonable principles and scientific methods must be obeyed to find out proper heterojunction candidates before real device implementation.

When developing heterojunction semiconductor devices, lattice mismatch at hetero-interface produces interface states and recombination[5]. Accordingly, ideal heterojunction materials to c-Si had better match the c-Si lattice, and thus this research begins from the lattice-matching materials. Among these materials, single-element material and binary compounds are preferred for minimizing the device fabrication complexity. **Table 1** lists the lattice-matching materials analyzed in this work, and most of them are III-V, II-VI compounds which have already been studied for many years and understood well. And experiences of developing these materials can also be utilized in the new devices proposed here. Next, the feasibilities of using these materials are further inspected according to the optimization criteria mentioned in previous section.

To obtain higher reflection barrier of minority carrier at the (*p*/*i*) interface, electrons here, *p*-layer requires higher conduction band, which suggests the electron affinity of *p*-layer material be lower

than that of a-Si:H (~3.8 eV). For higher barrier of minority carrier at the (*i*/*n*) interface, holes here, *n*-layer requires lower valence band, which indicates the sum of electron affinity and band gap of *n*-layer material be larger than that of a-Si:H (~5.5 eV). Based on these energy band selection standards and data listed in **Table 1**, proper heterojunction materials for *p*-region are selected as AlAs, or AlGaAs with low Ga content. Proper materials for *n*-region include GaP, AlP, InP, GaAs, ZnS, ZnSe, CdS. Amorphous Germanium is excluded for its energy band fails to satisfy. AlP is a highly reactive compound and not stable, so it is then excluded as well. Because large difference in coefficients of thermal expansion (CTE) during film epitaxial growth may deteriorate the film quality[11], materials with close CTE to c-Si are preferred. By these reasons, the compounds finally selected for *n*-layer are GaP, GaAs, ZnS. As all heterojunction materials selected for the new device are **compound** semiconductors, the novel c-Si heterojunction solar cell proposed in this work is denominated H**C**T (**H**eterojunction with **C**ompound **T**hin-layer).

Hence, we have preliminarily determined the hetero-materials used in novel HCT solar cells to replace a-Si:H films in HIT. In next section, the carrier transport mechanism and device theoretical efficiencies will be diagnosed in detail by device modeling, and HCT structures with better performance will be proposed.

It need clarify that the lattice-match is not a requisite for HCT cells. The development of HIT has demonstrated that high-efficiency cells can also be achieved by depositing amorphous thin film on c-Si. Therefore, this work does not deny the possibility of using lattice-mismatching, even amorphous-state materials as hetero-materials. The essentials of developing high-efficiency HCT cells will be concluded in the latter part of this paper.

3. Modeling investigation

The modeling investigation in this paper is implemented by employing wxAMPS which is a recently-developed solar cell simulation program[12]. It has incorporated two tunneling mechanisms, and the kernel algorithm is updated[13]. The numerical solution is obtained by solving three basic semiconductor equations (Poisson equation and continuity equations for electrons and holes), and is capable of revealing device inner information such as energy band, recombination profile and carrier distribution which are difficult to examine by experimental methods.

3.1 compound films/ c-Si interface

Several works have implemented numerical modeling studies on HIT solar cells[8,13,14]. Referred to previous works, a modeling parameter baseline for 24.7%-efficiency HIT cells was established at first by fitting the device experimental characteristics. The c-Si surface recombination velocity *S* obtained from the baseline simulation is ~0.6 cm/s, which is consistent with the real device with *S* of <2 cm/s[1]. By replacing a-Si:H with selected compound semiconductors and inputting corresponding parameters into the baseline, novel HCT structures are set up in the modeling and then simulated to verify if the efficiencies are improved. This section is focused on investigating the carrier transport at interfaces between compound films and c-Si surface, and the TCO contact is treated as Ohmic contact by assuming flat band condition in the simulation [15].

Physical Chemistry Chemical Physics Accepted Manuscript

Physical Chemistry Chemical Physics Accepted Manuscript

3.1.1 novel *p*-layers of compound thin films

The device performances when replacing a-Si:H(p) at the top with different *p*-layers are investigated at first. As mentioned previously, AlAs is a proper *p*-layer candidate. And for better comparison, *p*-type GaAs, InP, ZnS are also analyzed. The simulation here is concentrated on studying the effects of different interface energy band structures, and *p*-layer parameters such as doping density, defect states are assumed the same as those of a-Si:H(p) in the baseline.

Fig. 3a~3b illustrate device performances when a-Si:H(p) is replaced with different *p*-type compounds, and only AlAs(p) improves the device efficiency among the analyzed compounds,. This is because AlAs(p) increases the reflection barrier of electrons at the interface conduction band. The concentration of minority carriers arriving at *p*-layer is effectively decreased, and therefore the recombination in the *p*-layer emitter is shielded (seen in **Fig. 3c~3d**). In addition, with the same doping density, the work function of AlAs(p) is bigger than that of a-Si:H(p). The larger work function of *p*-layer increases the heterojunction built-in potential (V_{bi}) and enhances the photo-current collection. Furthermore, AlAs possesses wider band gap and is an indirect-band-gap material, which allows transmitting wider range of spectrum and reduces parasitic light absorption loss. By these reasons, the device short-circuit current (J_{sc}) is enhanced obviously. With respect to GaAs and InP, their work functions are smaller than that of AlAs, and they are direct-band-gap materials. Their effects are just opposite to those of AlAs, and consequently decrease J_{sc}. ZnS is a wide-band-gap material, but it introduces a too high blocking barrier of majority carriers at the interface valance band. As a result, the current transport at the hetero-interface is blocked, and most carriers recombine at the interface. In this case, J_{sc} is almost zero and the efficiency is extremely low.

3.1.2 novel *n*-layers of compound thin films

According to the simulation above, AlAs(p) is the best *p*-layer candidate among the analyzed compounds. Then, a-Si:H(n) at the rear side is replaced with different *n*-type compounds while setting AlAs(p) as the top *p*-layer. The doping density, defect states of *n*-layers are assumed the same as those of a-Si:H(n) in the baseline.

Seen from **Fig. 4a~4b**, device efficiencies are not raised when applying new *n*-layers at the bottom of HCT cells. As shown in **Fig. 4c**, except GaP(n), other *n*-type compounds do not effectively shield the recombination at the bottom heterojunction, and thereby device efficiencies decrease. In the case of GaAs(n), it does not increase the reflection barrier of holes at the interface valence band, the recombination at the heterojunction region increases and device efficiency drops obviously. ZnS(n) enlarges the reflection barrier and reduces the recombination at *n*-layer, but a little increases the recombination at the passivation layer. As a result, the device efficiency decreases slightly.

However, when HCT devices use c-Si(p) as substrate and novel *n*-layers are applied at the top, device J_{sc} and efficiencies can also increase noticeably (seen in **Table 2**). This is because the c-Si

Physical Chemistry Chemical Physics Accepted Manuscript

wafer has absorbs most of the light, and photo-carriers generated at the top of the cell is far more than those at the rear. And the recombination at the top is several orders of magnitude higher than that at the bottom, as shown in **Fig. 3c** and **Fig. 4c** in the case of c-Si(n) substrate. The carrier transport improvement by using new hetero-materials at the top hetero-interface effectively reduces the recombination therein, and hence improves J_{sc} more significantly. The carrier transport improvement at top hetero-interfaces can also be verified from quantum efficiency increments at short-wavelengths (seen in **Fig. 5**). It is also inspired by bifacial HIT modules[6] that HCT cells can also be developed as bifacial modules. In bifacial HCT that receives lights from both sides, the benefits of using novel hetero-structures at the top and the bottom will both exhibit.

The efficiency improvements in the modeling are consistent with the prediction given in previous paragraphs, and suggest several promising structures of high-efficiency HCT cells. As shown in **Table 2**, AlAs is the suitable *p*-layer material, and GaP, ZnS are proper *n*-layer materials.

3.1.3 Effects of compound film properties

There are lots of defect states in a-Si:H films deposited by PECVD (Plasma Enhanced Chemical Vapor Deposition), and the minority carrier diffusion length is at the order of 0.1 μm[16,17]. For high quality III-V compounds epitaxially grown by MOCVD (Metal Organic Chemical Vapor Deposition), the minority carrier diffusion length can reach 10 μm[18], and the density of defects can be as low as$10^{14\sim15}$ cm^{-3} [19], which is far below 2×10^{18} cm^{-3} used in the previous modeling. This indicates that film qualities of III-V compounds can be much better than those of a-Si:H, and the efficiency improvement is not limited to the results attained in previous simulation which is more focused on the effects of different energy band structures.

To study the influences of compound film properties on HCT device performances, the HCT structure of AlAs(p)/c-Si(n)/GaP(n) is simulated, and the top region which is more crucial to the device efficiency is investigated. As shown in **Fig. 6a**, device efficiency is not sensitive to the defect density and carrier mobilities of the AlAs(p) emitter. This is because the minority carrier reflection barrier enlarged by AlAs(p) has effectively reduced the electron concentration at *p*-layer, and the recombination therein is limited even all the electrons at *p*-layer recombine. When increasing the doping density, V_{bi} at the heterojunction gets higher which is beneficial to the device efficiency. But doping too heavily will result in larger recombination at *p*-layer and stop the trend of efficiency increasing. Therefore, there is an optimized doping density which is $10^{19}\sim10^{20}$ cm^{-3} given by this modeling.

The whole passivation layer lies in the space charge region (SCR), and the recombination in SCR constitutes the device recombination current that plays negative effects on V_{oc} and efficiency[5]. **Fig. 6b** shows that when the quality of the passivation layer is too bad (defect density over 10^{19} cm^{-3} or minority carrier mobility lower than 0.1 cm^2/Vs), the device performance deteriorates obviously.

Fig. 6c indicates that HCT is most sensitive to the c-Si surface quality, and the effects of surface recombination velocity S are significant. According to equation:

$$1/\tau_{eff} = 1/\tau_{bulk} + 2S/w \qquad \text{(Eq. 1)}$$

where τ_{eff} is the effective minority carrier lifetime which can be measured experimentally, τ_{bulk} is the minority carrier lifetime of the c-Si bulk (set as 130 ms in the modeling), w is the c-Si bulk thickness. The value of S is related to the interface defect density D_{it}. As revealed by the modeling, when D_{it} is 2.2x10^{13} cm^{-2}, S is 940 cm/s and τ_{eff} is reduced to 5 μs, and the device performance is seriously worsened. When D_{it} is 2.2x10^{5} cm^{-2}, S is 6x10^{-4} cm/s and τ_{eff} is as high as 128 ms, and the efficiency reaches 30.7%. In this case the bottleneck of device efficiency is no longer the surface recombination, but the c-Si bulk quality. When studying the ideal case in which no interface states at c-Si surface nor defects in the c-Si bulk, and there only exists radioactive recombination which generates black-body radiation, V_{oc} reaches ~900 mV and the Shockley-Queisser limit of c-Si solar cell efficiency, 31%[20], is achieved.

These modeling investigations demonstrate that, in order to obtain high-efficiency HCT cells with a certain hetero-structure, the c-Si surface passivation is the most important factor, the second is the quality of passivation layers, and the third is the optimized doping of the emitter. The ultimate efficiency of HCT solar cells is 31%.

3.2 The effects of TCO

According to the development of HIT solar cells, Ohmic contact is easily formed between *n*-type TCO and a-Si:H(n). But between the interface of TCO(n) and a-Si:H(p) would exist a Schottky-diode barrier which presents as an inverted junction, and the barrier height Φ_b is also one key factor determining the HIT device efficiency [7,21]. Similarly in HCT devices, the interface between TCO(n) and the *p*-type compound emitter may also suffer from the non-Ohmic contact resistance caused by this inverted junction. In this section, the contact resistance at the TCO(n)/emitter(p^+) interface and its effects on the HCT performance will be analyzed.

3.2.1 TCO/emitter interface

ITO (Indium Tin Oxide) is one of the most used TCO materials in HIT cells, and the HCT structure analyzed in this sub-section is based on ITO(n)/AlAs(p)/c-Si(n)/GaP(n). The ITO front contact is modeled by specifying the ITO/emitter surface recombination velocity as 1x10^{7} cm/s, and specifying the surface barrier height Φ_b according to different ITO work functions (Φ_{ITO})[15,21]. Depending on stoichiometry, oxidation type and deposition conditions, Φ_{ITO} varies between 4.3~5.5 eV[21,22].

Based on the parameters listed in **Table S1** in **SI**, the work function of a-Si:H(p) is about 5.4 eV, whereas the work function of AlAs(p) is higher, which is 5.66 eV. This means that AlAs(p) will increase Φ_b about 0.26 eV with the same Φ_{ITO}. The contact resistance of the surface barrier, R_c, can be evaluated by[23]:

$$R_c = \frac{q}{A^* kT} e^{\Phi_b / kT} \quad \text{(Eq. 2)}$$

where A^* is effective Richardson constant, q is electron charge, k is Boltzmann constant, and T is the temperature. According to Eq. 2, the contact resistance will increase greatly when using

Physical Chemistry Chemical Physics Accepted Manuscript

Physical Chemistry Chemical Physics Accepted Manuscript

AlAs(p) as the emitter.

Fig. 7 shows the simulation results of HIT and HCT device efficiencies under different Φ_{ITO}. In this simulation, the c-Si surface defect states D_{it} of HIT and HCT cells are both set as low as $2.2x10^5$ cm^{-2}. As shown in **Fig. 7**, the HCT efficiency starts to decrease when Φ_{ITO} is lower than 5.2 eV (Φ_b is 0.46 eV), and the HIT efficiency starts to decrease when Φ_{ITO} is lower than 5.0 eV (Φ_b is 0.4 eV). And when Φ_{ITO} is lower than 5.1 eV, the performance of HCT cells turns to be inferior to that of HIT cells. The modeling results implies that, when Φ_b <0.4 eV, the contact resistance of TCO/emitter(p^+) is neglectable compared with the series resistance of the c-Si bulk, and does not restrict the device efficiencies of HIT and HCT cells. However, when Φ_b is over ~0.5 eV, the contact resistance increases exponentially and becomes considerable. In this situation, fill factor (FF) and device efficiency deteriorate seriously, and JV curves even exhibit S-shape.

Therefore, Φ_{ITO} should be large enough to prevent the detrimental effects of high Φ_b. As seen in **Fig. 7,** Φ_{ITO} needs to be between 5.0~5.5 eV for HIT solar cells, and between 5.2~5.5 eV for HCT cells with the AlAs(p) emitter. The acceptable Φ_{ITO} range for HCT cells is narrower, so the TCO processing would become more challenging in the high-efficiency HCT device fabrication.

3.2.2 Alternative layer

In order to avoid the processing challenge in the TCO deposition, and meanwhile take full advantage of high mobilities of the selected compound materials, there is another scheme for the design of HCT cells: directly using the compound films as the alternative to TCO. For instance, above the AlAs(p) emitter, AlAs(p) (or AlGaAs(p) with some Ga doping) with a certain thickness can be deposited to reduce the sheet resistance of AlAs(p) and act as the conductive window layer.

For assuring a good lateral current collection between grid fingers, sheet resistance of the front conductive layer needs to be lower than 45 Ω/sq[24]. According to the carrier mobility and doping density of AlAs, the required thickness of AlAs window layer is estimated as ~200 nm. Although the band gap of AlAs is lower than that of ITO (3.8 eV), fortunately AlAs is the indirect-band-gap material and possesses low absorption coefficients. 200-nm-thick AlAs will not cause severe short-wavelength absorption loss, and the modeling results also verify this. Based on the simulation parameters used in **Fig. 7**, in the modeling when the thickness of the top AlAs(p) layer is increased from 10 nm to 200 nm, J_{sc} only decreases by 0.03 mA/cm^2, and the efficiency remains as high as 30.6% and only drops by 0.1%. Therefore, the HCT device in which TCO is replaced by AlAs(p) is also a practicable high-efficiency structure. Since the window layer and the emitter use the same material, another advantage of this structure is that the device fabrication process can be simplified. Furthermore, doping Ga into AlAs is able to increase the film conductivity and reduce the thickness with the same sheet resistance. But the Ga doping will simultaneously narrow the band gap and raise absorption coefficients[25]. So there will be an optimal Ga content and a film thickness if using AlGaAs(p) as the window layer.

Concerning the high-mobility *n*-type compound materials, GaP is also the indirect-band-gap material, and ZnS is a common window layer material for its wide band gap. Following similar

ideas, the TCO on the other side can also be replaced by adjacent *n*-type compounds so as to simplified the device fabrication and still maintain high efficiency. GaP(n), ZnS(n) of about 200-nm thick can be used to operate as the alternative window layer if applied at the top (when c-Si(p) is the substrate), or as the alternative conductive layer if applied at the rear (when c-Si(n) is the substrate).

Therefore, *p*-type and *n*-type compound films used in HCT devices can be deposited thicker to avoid the use of TCO, and then directly connected to the grids. In this alternative design of HCT structures, the non-Ohmic contact between TCO/emitter(p^+) is eliminated and the complexity of device fabrication is reduced, while high device efficiency is obtainable as well. Doping densities and film thicknesses of *p*-type and *n*-type compound layers can be further optimized to maximize the device performance.

4. Issues in device realization

There are some practical issues in realizing HCT devices. The intrinsic a-Si:H film with good passivation effects is deposited under 200 °C. But when developing III-V compounds such as GaP, AlAs by MOCVD, the growth temperatures are usually higher than 500 °C[26,27]. In such high temperatures, hydrogen will out-effuse from a-Si:H and the passivation effect will be degraded[28]. Therefore, intrinsic a-Si:H is not appropriate for the passivation layer of HCT, and new passivation materials and approaches have to be searched.

So far, passivation materials used in c-Si homojunction solar cell include SiN_x, Al_2O_3, SiO_2, and their combination[29]. But these materials have wide band gaps and are similar to insulator. In the processing of c-Si homojunction solar cells, these passivation layers usually need etching to have grid material intimately contact c-Si[2]. If applying these materials as passivation layers in HCT, large blocking barrier will be introduced at hetero-interfaces, and photocurrent is not able to get through. Therefore, these passivation materials used in homojunction solar cell are not compatible to the case of HCT.

One ideal solution is that the compounds themselves, such as AlAs, GaP, have passivation effects on c-Si and are capable of achieving good passivation. There have been plenty of researches on growing III-V compounds on Si substrate, but people are focused on influences of Si substrate on III-V materials and devices. Few efforts are put in studying the effects of III-V films on the c-Si surface. Previous work tried to apply ZnS, GaP as window layers to c-Si homojunction solar cells[30], in which device quantum efficiencies at short-wavelengths increased, and the passivation effects produced by these two compounds did are observed. Different from the traditional thoughts of developing III-V, II-VI compounds, this work pays attention to the passivation effects of compound films on c-Si, and aims to apply the effects to realizing high-efficiency HCT devices. This will be a meaningful research topic of great interest and novelty.

It is commonly agreed that high quality III-V compounds are hard to grow on Si substrate[11]. But in design principles of HCT, high quality crystalline materials are not prerequisite for HCT devices, just as HIT cells utilize amorphous materials and also achieve high efficiency. Referring to

Physical Chemistry Chemical Physics Accepted Manuscript

previous works[31,32] and the equation of estimating critical thickness t_c [33],

$$t_c \approx a_{Si} / 2 | f | \quad \text{(Eq. 3)}$$

where a_{si} is lattice constant of c-Si, f is lattice misfit, the critical thickness of each selected compound epitaxially grown on c-Si can be given as: AlAs ~6 nm, GaP ~90 nm, ZnS ~70 nm. If using these compound films as the passivation layers which could be intrinsic materials and around 5-nm thick, the whole passivation layer will be thinner than the critical thickness. Thus, the misfit dislocation will not occur within the passivation layer, and this is quite beneficial to the formation of high-quality passivation layers and the reduction of interface defect states. The dislocation would not exist in the GaP or ZnS emitters, but might be generated in the AlAs(p) emitter. But based on previous modeling studies, HCT cell efficiencies are not sensitive to the crystalline quality of the AlAs(p) emitter. Therefore, the dislocation in the emitter will not restrict the device efficiency. As long as the emitter layers are properly doped, favorable energy band structures are formed at hetero-interfaces, and excellent surface passivation is assured, high-efficiency HCT solar cells can be achieved.

At present, there are also many researches trying to use alternative hetero-materials to replace a-Si:H[10,34,35], e.g., using μc-Si, or doping some elements (such as O, C) into a-Si:H films in order to improve the passivation, increase the band gap and reduce parasitic absorption loss. However, these materials are still limited to the a-Si:H-based concept, and do not bring in the better energy band structure depicted in **Fig. 2b**. So far, the highest efficiencies of the cells using these materials have not exceeded that of HIT cells (listed in **Table 3**). For instance, the use of a-SiO:H increases the top layer band gap and reduces the parasitic absorption, as a result J_{sc} increases slightly. But its lower valence band enlarges the valence band offset at the a-SiO:H(p/i)/c-Si(n) interface, and worsen the interface transport of the majority carrier, holes here. Consequently, FF is reduced and the final efficiency is 0.4% lower than that of the HIT device using a-Si:H[10]. The results can be explained by the theory used in this work. Compared with these a-Si:H-based hetero-materials, the III-V, II-VI compounds used in HCT cells are able to establish better interface band structures, and allow to realize higher device efficiency.

III-V solar cells are also applied on top of Si solar cell to form tandem solar cells[19,26,36,37]. But III-V solar cells of several-micron-thickness are far beyond the critical thickness and vulnerable to the effects of Si substrate, and the reported highest efficiency of III-V/Si tandem structure is 21.4%[19]. The HCT concept in this work is to grow III-V compounds of nanometers on c-Si to form heterojunction solar cells that are still capable of achieving high efficiency and potentially better than HIT. The HCT development can make use of existing facilities of III-V/Si tandem solar cells, but the processing complexity and cost are greatly saved.

5. Summary

Through theoretical analysis and design, novel HCT solar cells have been proposed in this work. The concept is to improve interface carrier transport by introducing wider-band-gap compound films with more appropriate energy band structure, and thereby enhances the cell efficiency. This work preliminarily selects the compounds from binary semiconductors whose lattice constants, energy

Physical Chemistry Chemical Physics Accepted Manuscript

Physical Chemistry Chemical Physics Accepted Manuscript

bands and coefficients of thermal expansion match the ones of c-Si. And after modeling investigation, the suitable compounds are AlAs used in the *p*-layer, and GaP, ZnS used in the *n*-layer. There are two schemes for the HCT structures: one is based on the HIT structure and just replaces a-Si:H with the selected compounds. This scheme has a stricter requirement for the TCO fabrication. The other is to replace both a-Si:H and TCO with the compound films. This scheme avoids the non-Ohmic contact at the TCO(n)/emitter(p^+) interface and simplifies the device processing, and high efficiency is still obtainable.

The critical factor in high-efficiency HCT devices is the c-Si surface passivation, and the second is the quality of the passivation layer. The device efficiency is not sensitive to the defect states or carrier mobilities of the compound emitters, but the emitters should be properly doped. The ultimate theoretical efficiency of HCT is 31%. In HCT solar cells, a-Si:H is not the compatible passivation material, and it will be a meaningful research subject to investigate the passivation effects of III-V, II-VI compounds on the c-Si surface.

It has been more than 20 years efforts to achieve 24.7%-efficiency HIT cells since the HIT concept was first proposed. Similarly, it also requires plenty of work to actualize the HCT advantages predicted in this work. Once the concept is validated by experimental efforts, this work will revolutionarily influence the development of c-Si heterojunction solar cells, and open a new era of searching better hetero-materials for the application of high-efficiency c-Si solar cells.

Acknowledgements

The authors would like to thank the support of 973 National Basic Research Program of China (BE091571), and National Natural Science Foundation of China (61076061, 61274053).

Supplementary information

The supplementary information includes a detailed introduction of carrier transport mechanism at heterojunction interface, describes the modeling set-up in wxAMPS and numerical evaluation of surface recombination velocity, and lists material parameters used in the simulation.

References:

1. Taguchi, M. *et al.* 24.7% Record Efficiency HIT Solar Cell on Thin Silicon Wafer. *IEEE J. Photovoltaics* (2013).

2. Tobías, I., Cañizo, C. & Alonso, J. in *Handb. Photovolt. Sci. Eng.* (2003).

3. Poortmans, J., Ghannam, M., Abdulraheem, Y. & Shehadah, G. BASIC UNDERSTANDING OF THE ROLE OF THE INTERFACIAL INVERSION LAYER IN THE OPERATION. in *28th EU-PVSEC* 822–826 (2013).

4. Taguchi, M., Terakawa, A., Maruyama, E. & Tanaka, M. Obtaining a higher Voc in HIT cells. *Prog. Photovoltaics Res. Appl.* **13,** 481–488 (2005).

5. Fonash, S. *Solar Cell Device Physics*. (Academic Press, 2010).

6. Mishima, T., Taguchi, M., Sakata, H. & Maruyama, E. Development status of high-efficiency HIT solar cells. *Sol. Energy Mater. Sol. Cells* **95,** 18–21 (2011).

7. Kanevce, A. & Metzger, W. K. The role of amorphous silicon and tunneling in heterojunction with intrinsic thin layer (HIT) solar cells. *J. Appl. Phys.* **105,** 094507 (2009).

8. Zhao, L., Zhou, C. L., Li, H. L., Diao, H. W. & Wang, W. J. Design optimization of bifacial HIT solar cells on p-type silicon substrates by simulation. *Sol. Energy Mater. Sol. Cells* **92,** 673–681 (2008).

9. Shen, L., Meng, F. & Liu, Z. Roles of the Fermi level of doped a-Si:H and band offsets at a-Si:H/c-Si interfaces in n-type HIT solar cells. *Sol. Energy* **97,** 168–175 (2013).

10. Peter Seif, J. *et al.* Amorphous silicon oxide window layers for high-efficiency silicon heterojunction solar cells. *J. Appl. Phys.* **115,** 024502 (2014).

11. Olson, J., Friedman, D. & Kurtz, S. High-efficiency III-V multijunction solar cells. *Handb. Photovolt. Sci. Eng.* (2003). at <https://web.engr.oregonstate.edu/~yokochia/wiki/uploads/Documents/CH09 3-5 cells.pdf>

12. Liu, Y., Sun, Y. & Rockett, A. A new simulation software of solar cells—wxAMPS. *Sol. Energy Mater. Sol. Cells* **98,** 124–128 (2012).

13. Liu, Y., Sun, Y. & Rockett, A. An improved algorithm for solving equations for intra-band tunneling current in heterojunction solar cells. *Thin Solid Films* **520,** 4947–4950 (2012).

14. Hernández-Como, N. & Morales-Acevedo, A. Simulation of hetero-junction silicon solar cells with AMPS-1D. *Sol. Energy Mater. Sol. Cells* **94,** 62–67 (2010).

15. Stangl, R., Froitzheim, A., Schmidt, M. & Fuhs, W. Design criteria for amorphous/crystalline silicon heterojunction solar cells-a simulation study. *Proc. 3rd World Conf. Photovolt. Energy Convers.* **2,** 3–6 (2003).

16. Beck, N., Wyrsch, N., Hof, C. & Shah, A. Mobility lifetime product — A tool for correlating a -Si: H film properties and solar cell performances. *J. Appl. Phys.* **79,** 9361–9368 (1996).

17. Serin, T. & Serin, N. Determination of electron-diffusion length from photocurrent characteristics of the structure ITO/a-SiC: H (p-type)/a-Si: H/a-Si: H (n-type)/Pd. *Appl. Phys. A* **431433,** 1–3 (1994).

18. Schubert, E. F. Room temperature properties of semiconductors: III–V phosphides Quantity. *http://homepages.rpi.edu/~schubert/Educational-resources/Materials-Semiconductors-III-V-phosphides.pdf* **1,** 1

Physical Chemistry Chemical Physics Accepted Manuscript

19. Umeno, M., Soga, T., Baskar, K. & Jimbo, T. Heteroepitaxial technologies on Si for high-efficiency solar cells. *Sol. Energy Mater. Sol. Cells* **50,** 203–212 (1998).

20. Shockley, W. & Queisser, H. Detailed Balance Limit of Efficiency of p-n Junction Solar Cells. *J. Appl. Phys.* **32,** (1961).

21. Centurioni, E. & Iencinella, D. Role of front contact work function on amorphous silicon/crystalline silicon heterojunction solar cell performance. *IEEE Electron Device Lett.* **24,** 177–179 (2003).

22. Schlaf, R., Murata, H. & Kafafi, Z. . Work function measurements on indium tin oxide films. *J. Electron Spectros. Relat. Phenomena* **120,** 149–154 (2001).

23. Gunawan, O., Todorov, T. K. & Mitzi, D. B. Loss mechanisms in hydrazine-processed Cu2ZnSn(Se,S)4 solar cells. *Appl. Phys. Lett.* **97,** 233506 (2010).

24. Barraud, L. *et al.* Hydrogen-doped indium oxide/indium tin oxide bilayers for high-efficiency silicon heterojunction solar cells. *Sol. Energy Mater. Sol. Cells* **115,** 151–156 (2013).

25. Adachi, S. GaAs, AlAs, and AlxGa1−xAs Material parameters for use in research and device applications. *J. Appl. Phys.* **58,** R1 (1985).

26. Soga, T., Kato, T., Umeno, M. & Jimbo, T. Photovoltaic properties of an Al x Ga 1-x As solar cell (x= 0–0.22) grown on Si substrate by metalorganic chemical vapor deposition and thermal cycle annealing. *J. Appl. Phys.* (1996).

27. Huang, S. R., Lu, X., Wang, X. & Opila, R. L. WINDOWLAYER PROPERTIES OF GaP FILMS GROWN ON Si BY LIQUID PHASE EPITAXY. in *Photovolt. Spec. Conf.* 7–10 (2008).

28. Li, H. & Wenham, S. Influence of a-Si: H deposition power on surface passivation property and thermal stability of a-Si: H/SiNx: H stacks. *IEEE J. Photovoltaics* **2,** 405–410 (2012).

29. Rahman, M. Z. & Khan, S. I. Advances in surface passivation of c-Si solar cells. *Mater. Renew. Sustain. Energy* **1,** 1 (2012).

30. Landis, G. a. *et al.* Wide-bandgap epitaxial heterojunction windows for silicon solar cells. *IEEE Trans. Electron Devices* **37,** 372–381 (1990).

31. Soga, T., Jimbo, T. & Umeno, M. Dislocation generation mechanisms for GaP on Si grown by metalorganic chemical vapor deposition. *Appl. Phys. Lett.* **63,** 2543–2545 (1993).

32. Hull, R. & Fischer-Colbrie, a. Nucleation of GaAs on Si: Experimental evidence for a three-dimensional critical transition. *Appl. Phys. Lett.* **50,** 851 (1987).

Physical Chemistry Chemical Physics Accepted Manuscript

33. Nam, S., Byungsung, O. & Lee, K. Growth and Structural Properties of ZnS / GaAs and ZnS / GaP Epilayers by Hot-Wall Epitaxy. **33,** 309–312 (1998).

34. Lien, S.-Y., Wu, B.-R., Liu, J.-C. & Wuu, D.-S. Fabrication and characteristics of n-Si/c-Si/p-Si heterojunction solar cells using hot-wire CVD. *Thin Solid Films* **516,** 747–750 (2008).

35. Pysch, D., Bivour, M., Hermle, M. & Glunz, S. W. Amorphous silicon carbide heterojunction solar cells on p-type substrates. *Thin Solid Films* **519,** 2550–2554 (2011).

36. Kotulak, N. A. GROWTH AND ANALYSIS OF GALLIUM PHOSPHIDE ON SILICON FOR VERY HIGH EFFICIENCY SOLAR CELL. (2011).

37. García-Tabarés, E. & Garcia, I. Integration of III-V materials on silicon substrates for multi-junction solar cell applications. *Proc. 8th Spanish Conf. Electron Devices* (2011). at <http://ieeexplore.ieee.org/xpls/abs_all.jsp?arnumber=5744190>

38. D W Palmer. Semiconductors Information. *www.semiconductors.co.uk* (2006).

39. Ber, N. U. M. Electrical and Optical Properties of Amorphous Germanium. **254,** (1966).

40. Kazuyoshi Nakada and Makoto Konagai. APPLICATION OF INTRINSIC AMORPHOUS SILICON OXIDE FILMS AS PASSIVATION LAYERS for textured heterojunction solar cell. in *27th Eur. Photovolt. Sol. Energy Conf. Exhib.* 1616 – 1618 (2012).

41. Magafas, L. Electrical properties of a-SiC/c-Si (p) heterojunctions. *Semicond. Sci. Technol.* **7,** 1363 (1992).

Physical Chemistry Chemical Physics Accepted Manuscript

Table 1. Parameters of lattice-matching semiconductors to c-Si [14,18,38,39]

	Lattice constant (Å)	**Electron affinity (eV)**	**Band gap (eV)**	**Coefficient of thermal expansion (10^{-6}/K)**
c-Si	5.43	4.01	1.11I	2.33
III-V				
GaP	5.45	3.8	2.26I	5.3
AlP	5.46	3.98	2.45 I	N.A.
GaAs	5.65	4.07	1.42D	5.8
AlAs	5.66	3.5	2.16I	3.5
InP	5.87	4.5	1.35D	4.5
II-VI				
ZnS	5.41	3.9	3.68D	6.5
ZnSe	5.67	4.09	2.82D	7.6
CdS	5.82	4.2	2.4D	N.A.
Amorphous				
a-Si	N.A.	3.8	1.7	N.A.
a-Ge	N.A.	4.0	1.1	N.A.

Note：

I：indirect band gap; D: direct band gap

N.A.: not available

Physical Chemistry Chemical Physics Accepted Manuscript

Table 2. Modeled device performances with different HCT structures. Each compound film is assumed to have the same doping density and defect states as a-Si:H. Detailed simulation parameters for each layer are listed in **Table S1** in SI.

Structure	Voc(V)	Jsc(mA/cm^2)	FF (%)	η (%)
a-Si:H(p)/c-Si(n)/a-Si:H(n) (baseline)	0.744	39.3	84.5	24.7
c-Si(n) as substrate				
GaAs(p)/c-Si(n)/a-Si:H(n)	0.742	38.2	84.4	24.0
InP(p)/c-Si(n)/a-Si:H(n)	0.746	37.9	84.9	24.0
AlAs(p)/c-Si(n)/a-Si:H(n)	0.746	41.1	84.7	26.0
AlAs(p)/c-Si(n)/GaP(n)	0.746	41.1	84.7	26.0
AlAs(p)/c-Si(n)/GaAs(n)	0.705	41.0	82.2	23.7
AlAs(p)/c-Si(n)/ZnS(n)	0.739	41.1	84.6	25.7
c-Si(p) as substrate				
a-Si:H(n)/c-Si(p)/a-Si:H(p)	0.743	38.6	84.6	24.2
GaP(n)/c-Si(p)/a-Si:H(p)	0.745	40.7	84.5	25.6
GaP(n)/c-Si(p)/AlAs(p)	0.748	40.7	84.8	25.8
GaAs(n)/c-Si(p)/AlAs(p)	0.703	37.8	81.8	21.7
ZnS(n)/c-Si(p)/AlAs(p)	0.739	40.5	84.8	25.3

Physical Chemistry Chemical Physics Accepted Manuscript

Table 3 Device efficiencies when incorporating other a-Si:H-based hetero-materials into HIT solar cells

Hetero-material	$\Delta\chi$ (eV)*	ΔE_g (eV)[#]	Device structure	Efficiency (%)
a-SiO:H	0	+0.2	a-Si:H(p)/a-SiO:H(i)/c-Si(n)/a-Si:H(i)/a-Si:H(n^+)	20.4[10]
			μc-SiO:H(p)/a-SiO:H(i)/c-Si(n)/a-SiO:H(i)/a-Si:H(n^+)	20.1[40]
a-SiC:H	+0.3[41]	+0~0.5[35]	a-SiC:H(n)/a-Si:H(i)/c-Si(p)	18.5[35]
μc-Si	0	-0.4	μc-Si:H(n)/a-Si:H(i)/c-Si(p)/a-Si:H(i)/μc-Si:H(p^+)	16.4[34]

* the electron affinity variation compared with that of a-Si:H

[#] the band gap variation compared with that of a-Si:H

Physical Chemistry Chemical Physics Accepted Manuscript

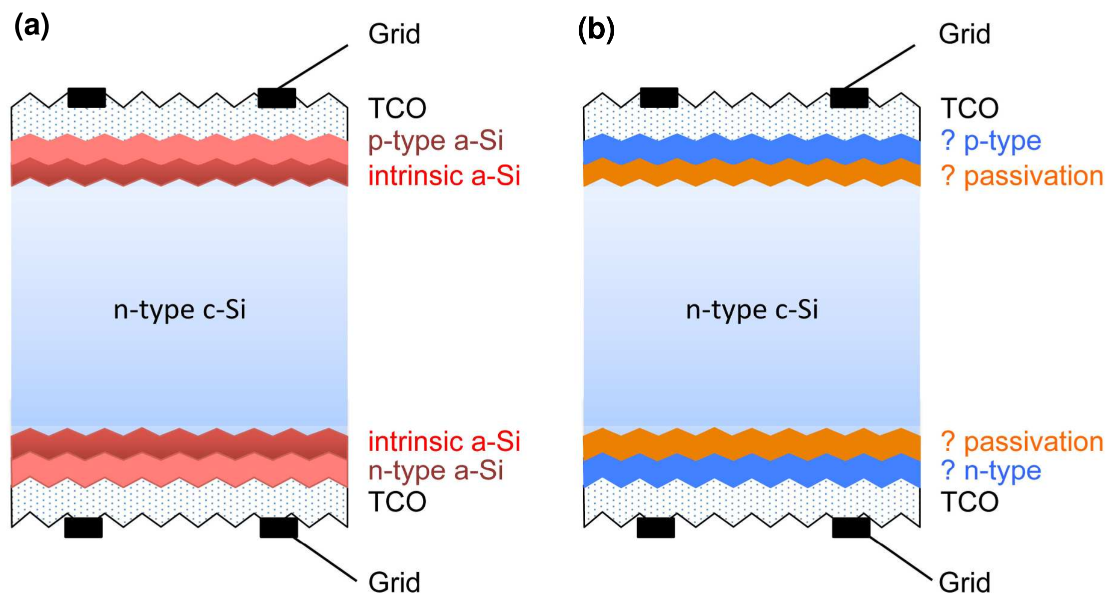

Figure 1 **(a)** cross-section schematic of HIT solar cells. A typical structure of HIT is: grids/Transparent Conductive Oxide (TCO)/a-Si:H(p)/a-Si:H(i)/c-Si(n)/a-Si:H(i)/a-Si:H(n^+)/TCO/grids. The *n*-type c-Si is the light absorber and usually 50~300 μm thick. The *p*-type, *n*-type a-Si:H thin films at both sides are 5~10 nm thick and heavily doped. The top a-Si:H layer acts as the emitter, and the rear a-Si:H layer contributes to the back-surface-field (BSF). The intrinsic a-Si:H between doped a-Si:H and c-Si is introduced as a buffer layer to passivate surface defects of c-Si and reduce interface carrier recombination. The passivation quality is crucial to the device open-circuit voltage (V_{oc}) and conversion efficiency**.** **(b)** cross-section schematic of novel c-Si heterojunction solar cells.

Physical Chemistry Chemical Physics Accepted Manuscript

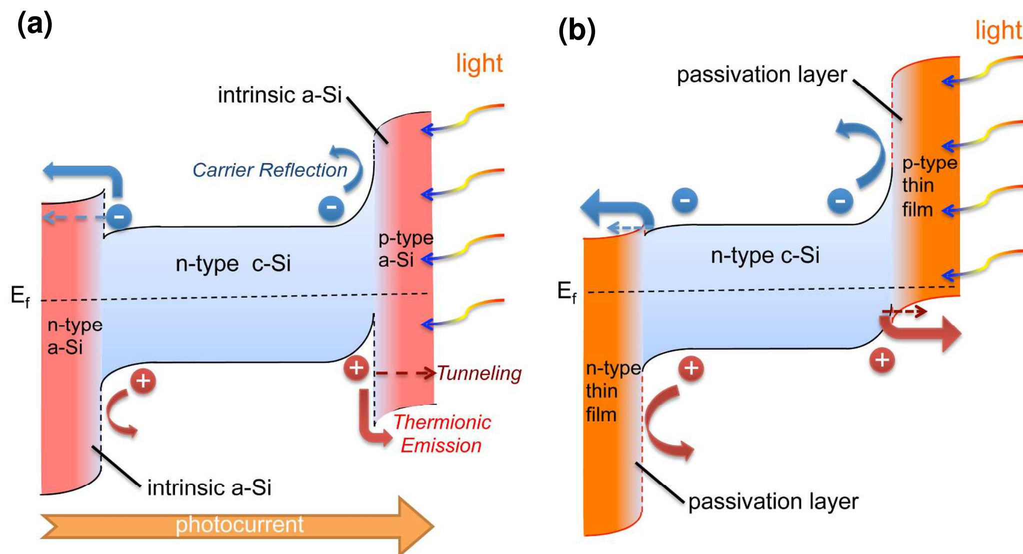

Figure 2 **(a)** energy band diagram of HIT solar cells. E_f is the Fermi level at thermal equilibrium. At the (*i/n*) hetero-interface shown on the left, the minority carrier is hole and the majority carrier is electron. Whereas the (*p/i*) hetero-interface shown on the right is strongly inverted by the large band bending, and here the minority carrier becomes electron and the majority carrier is hole. At each interface, the conduction/valence band offsets form one favorable reflection barrier of minority carrier and one unfavorable blocking barrier of majority carrier. Majority carriers have to transport through the blocking barriers by thermionic emission as well as the tunneling mechanism (represented by dotted arrows). **(b)** a more ideal energy band diagram of c-Si heterojunction solar cells, in which reflection barriers are raised higher and blocking barriers are reduced lower (see S2 in **SI** for more information on the carrier interface transportation).

Physical Chemistry Chemical Physics Accepted Manuscript

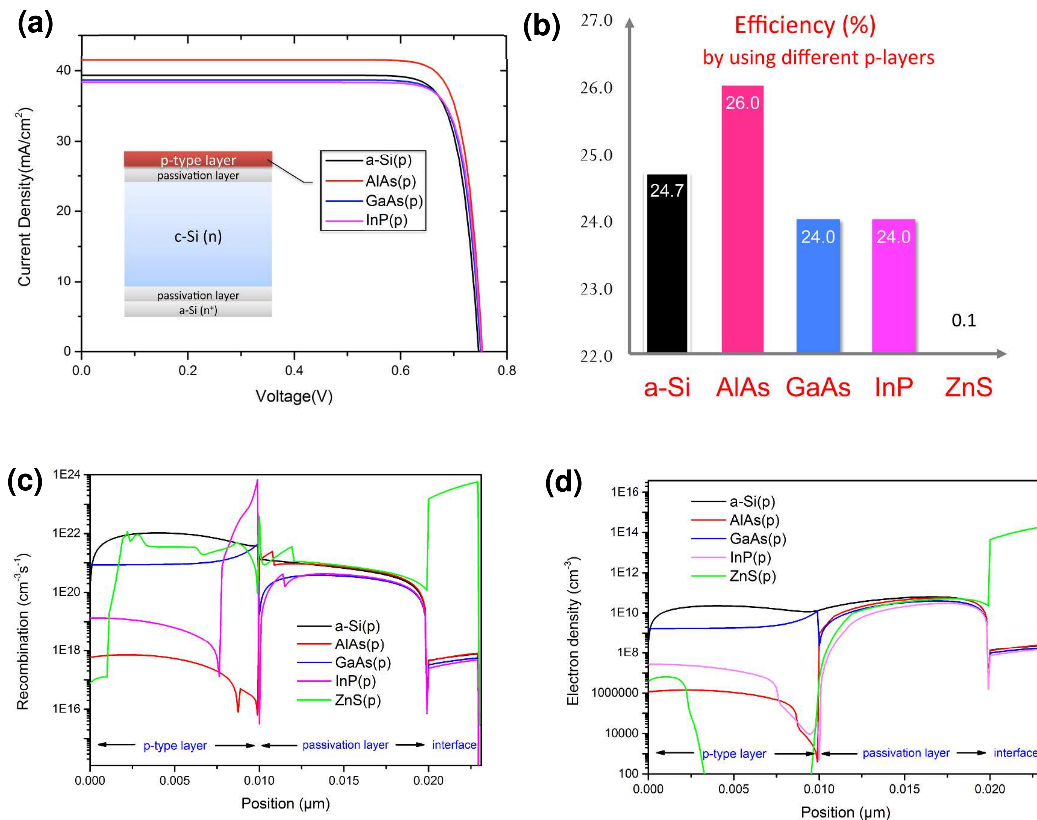

Figure 3 (**a**) modeled current-voltage curves of HCT cells using different *p*-layer compounds at the top. The device performance of world-record 24.7%-efficiency HIT cell is used as reference. (**b**) power conversion efficiencies of HCT cells with different *p*-layers. (**c**) recombination rates at (*p*/*i*) interfaces with different *p*-layers. (**d**) profiles of the minority carrier (electron) at (*p*/*i*) interfaces with different p-layers.

Physical Chemistry Chemical Physics Accepted Manuscript

Physical Chemistry Chemical Physics Accepted Manuscript

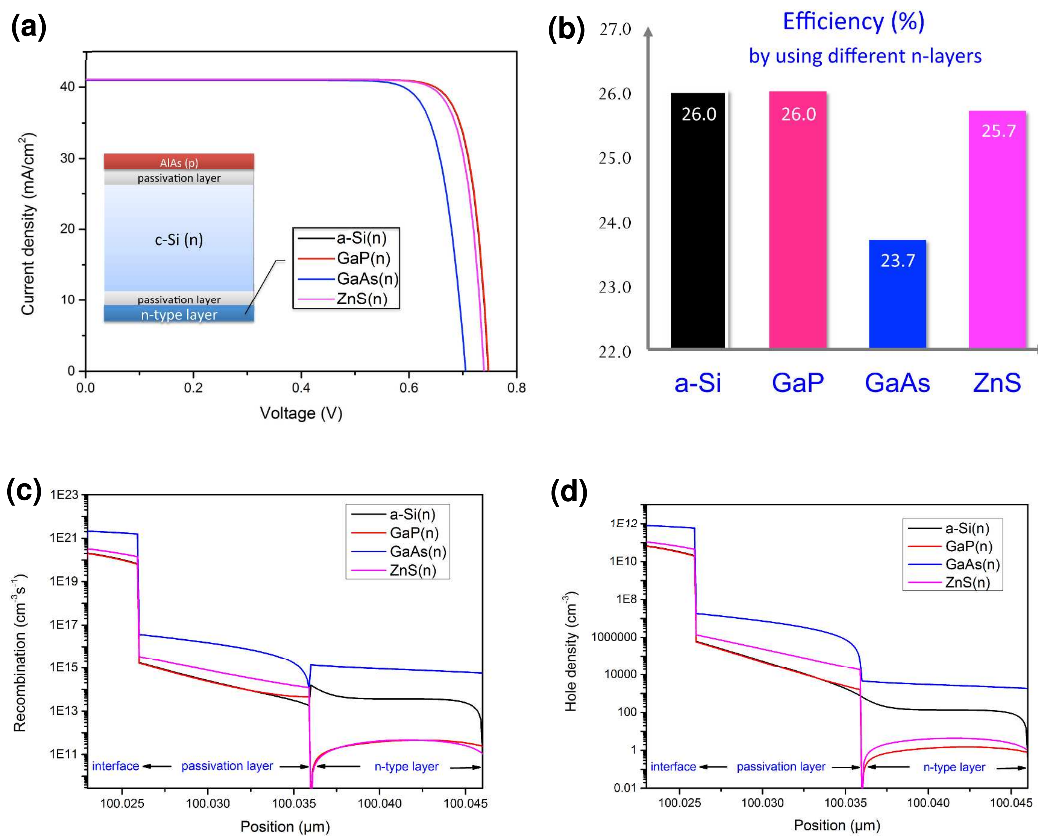

Figure 4 **(a)** modeled current-voltage curves of HCT cells using different *n*-layer compounds at the rear side. AlAs(p) is set as the top *p*-layer. **(b)** power conversion efficiencies of HCT cells with different *n*-layers. **(c)** recombination rates at (*i*/*n*) interfaces with different *n*-layers. **(d)** profiles of the minority carrier (hole) at (*i*/*n*) interfaces with different *n*-layers.

Physical Chemistry Chemical Physics Accepted Manuscript

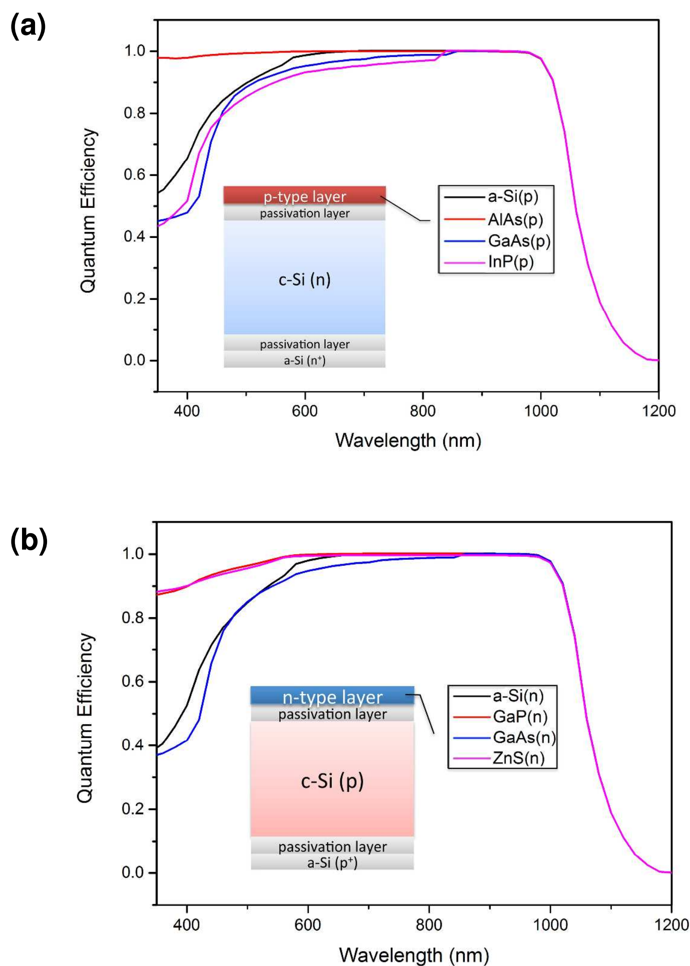

Figure 5 **(a)** modeled quantum efficiencies of HCT with c-Si(n) substrate by using different top *p*-layers. **(b)** modeled quantum efficiencies of HCT with c-Si(p) substrate by using different top *n*-layers. In the modeling, the top layers are as thin as 10 nm, and their optical influences are not significant. The quantum efficiency increments at short-wavelengths are mainly attributed to electrical improvements, which are carrier transport enhancement resulted by using novel compound hetero-materials at top hetero-interfaces.

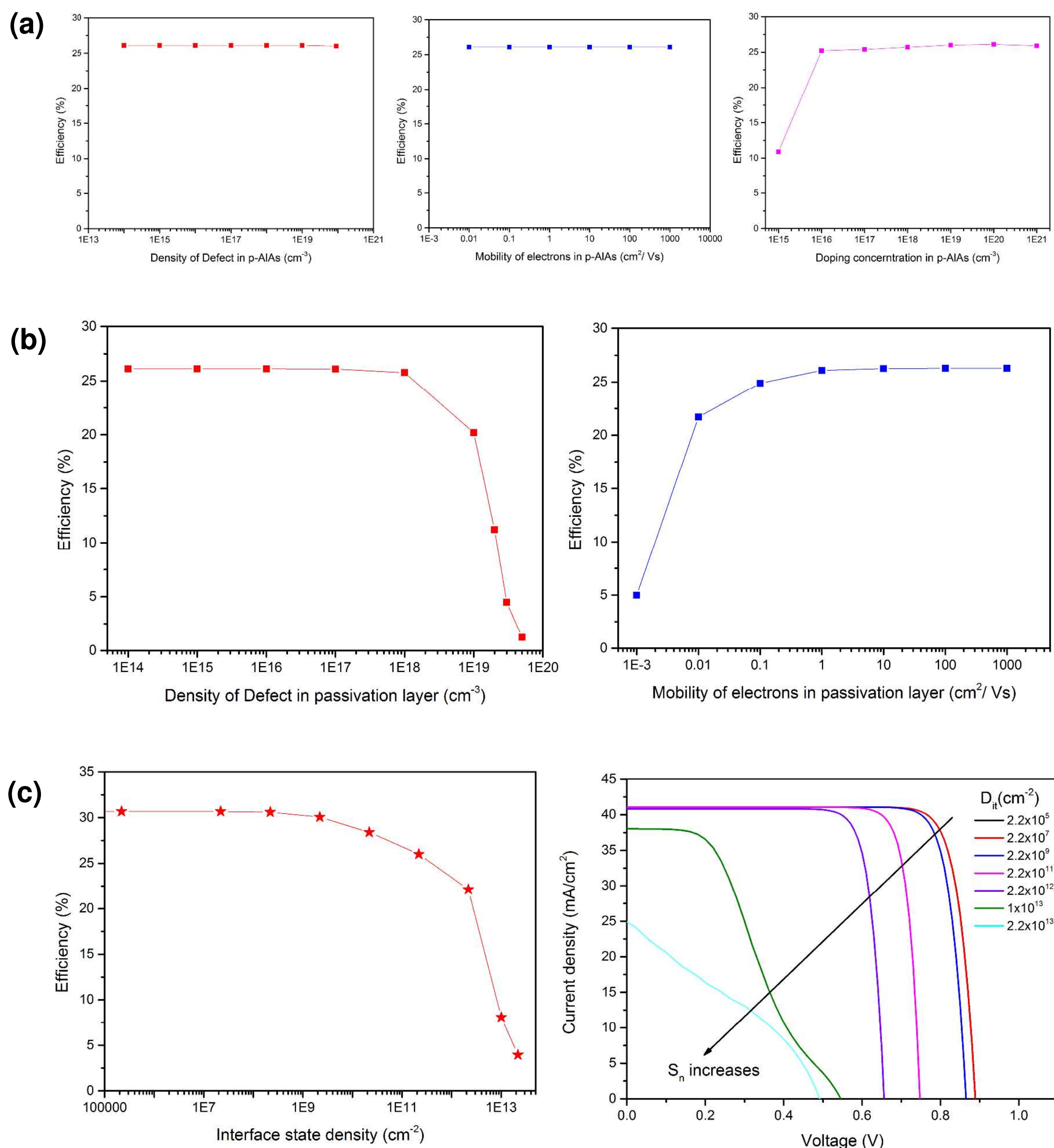

Figure 6 (**a**) the sensitivity of device efficiency to AlAs(p) film properties. The properties include defect density N_t, doping density N_a, carrier mobilities of electrons and holes μ_n, μ_p. The parameter baseline is N_t=1x10^{15} cm^{-3}, N_a=1x10^{20} cm^{-3}, μ_n=200 cm^2/Vs. When effects of one parameter are studied, only this parameter is swept and other parameters are kept as the baseline values. The hole mobility follows the relation $\mu_p = \mu_n/2$. **(b)** the effects of passivation layer properties. The properties include defect density and carrier mobilities. **(c)** the effects of c-Si surface quality. The surface quality is represented by D_{it}. In the current-voltage curves, the red line and black line almost overlap, as in these cases S is so low that the efficiency turns to be limited by the quality of the c-Si bulk.

Physical Chemistry Chemical Physics Accepted Manuscript

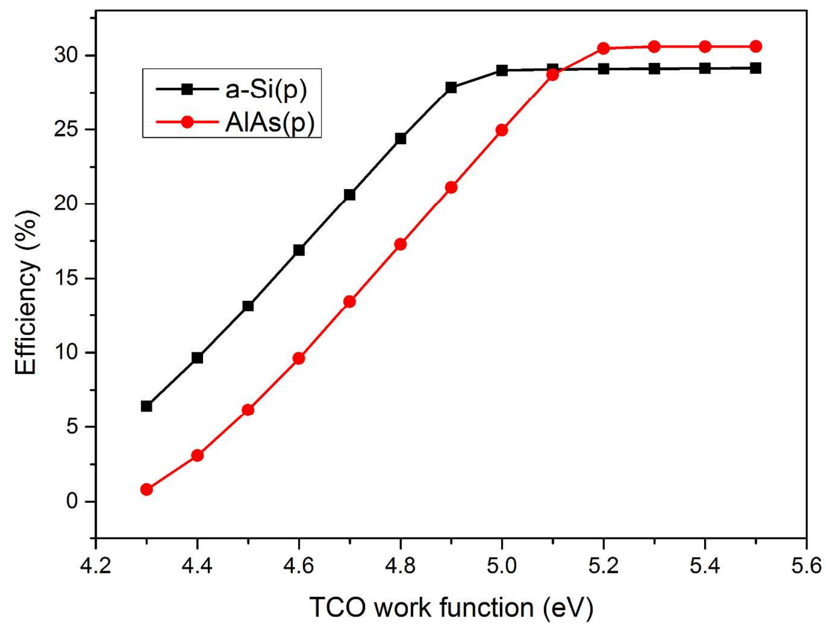

Figure 7 efficiencies of HIT (a-Si:H(p) as the emitter) and HCT (AlAs(p) as the emitter) solar cells vs. the work function of ITO.

Physical Chemistry Chemical Physics Accepted Manuscript